

Magnetic order and exchange interactions in monoatomic 3d transition-metal chains

Y. Mokrousov,^{1,*} G. Bihlmayer,² S. Blügel,² and S. Heinze¹

¹*Institute for Applied Physics, University of Hamburg, 20355 Hamburg, Germany*

²*Institut für Festkörperforschung, Forschungszentrum Jülich, D-52425 Jülich, Germany*

(Received 20 November 2006; published 19 March 2007)

Based on first-principles calculations we analyze the magnetic order and the exchange interactions in monoatomic 3d transition-metal chains of V, Cr, Mn, Fe, and Co. While freestanding Fe and Co chains remain ferromagnetic in the entire range of interatomic distances, V, Cr, and Mn chains change their magnetic state from antiferromagnetic (AFM) to ferromagnetic (FM) upon stretching. The corresponding distance-dependent exchange interaction is in striking resemblance to the Bethe-Slater curve. We demonstrate that in combination with the symmetry reduction on the (110) surfaces of Cu, Pd, Ag, and NiAl even a weak chain-surface hybridization is sufficient to dramatically change the magnetic coupling in the chains. In particular, we find a tendency towards antiferromagnetic coupling. The obtained magnetic state of a specific chain depends sensitively on the chemical composition and the lattice constant of the surface. Surprisingly, Cr and Mn chains show a transition from ferromagnetic coupling in freestanding chains to antiferromagnetic coupling on the (110) surfaces of Pd, Ag, and NiAl. For Fe and Co chains on NiAl(110) the FM and AFM states differ by only 2 meV, suggesting the possibility of a more complex, noncollinear magnetic ground state.

DOI: [10.1103/PhysRevB.75.104413](https://doi.org/10.1103/PhysRevB.75.104413)

PACS number(s): 73.63.Nm, 73.20.-r, 75.75.+a

I. INTRODUCTION

Driven by the dream of atomic-scale storage devices and spin-based computational schemes, magnetism in artificially created one-dimensional (1D) structures such as metallic wires is currently a topic of intense interest. While the fabrication of such structures is obviously a tremendous experimental challenge, the theoretical understanding is much more difficult than the simple structure of the systems suggests. Being at the boundary between the physics of itinerant electrons in bulk and localized electrons in molecules, chains are a fruitful playground for testing the validity and limitations of models characteristic of both branches. Especially striking are the consequences of 1D physics for magnetism in these systems. Electrons, which are confined in two dimensions and restricted in their dynamics to the remaining one, compensate the reduced hopping due to less neighboring atoms by favoring exchange. This leads to nonzero magnetization not only in chains of most transition metals, but even in *sp* metals¹—for example, Al.² This strong tendency towards magnetism not only makes them promising candidates and model systems in the field of nanoscale magnetism and spintronics, but also stimulates a profound theoretical quest to revise well-known concepts in magnetism.

In their pioneering experiments³ Gambardella *et al.* demonstrated ferromagnetic order and enhanced magnetic anisotropy of monoatomic Co chains on a stepped Pt(111) surface. Numerous theoretical studies followed this experiment, focusing primarily on the unusual magnetic anisotropy in this particular system.^{4–6} Some studies also considered magnetism and magnetic order of 4d and 5d transition-metal monoatomic chains.^{7–9} Experimentally, the fabrication of such 1D structures is extremely difficult since either atom manipulation or self-assembly techniques are involved. For the latter only a few other examples exist until now. For example, monoatomic Co chains on Pd(110) (Ref. 10) and biatomic Fe chains on the reconstructed (100) surface of Ir (Ref. 11) have

been created. While these systems are assumed to couple ferromagnetically, more recently, there has been increasing interest in antiferromagnetic order. In a key experiment, Hirjibehedin *et al.*¹² suggested antiferromagnetic coupling in linear chains from two to ten Mn atoms created by atom manipulation on an insulating CuN/Cu(001) surface. An excellent description of the magnetic properties based on the Heisenberg model was possible due to the localized nature of the magnetic moments. On the other hand, ferromagnetism in Mn dimers on NiAl(110) has been reported,¹³ demonstrating the crucial impact of the surface on the exchange interactions.

Clearly, the surface composition, symmetry, and electronic properties as well as the interatomic distance in the chain could be equally important for the magnetic coupling between the chain atoms. In two-dimensional systems—i.e., ultrathin films—the competition of ferromagnetic and antiferromagnetic coupling, which can give rise to complex magnetic order, has been extensively investigated in the past but still new surprises are reported (see, e.g., Ref. 14). Concerning monoatomic wires, few studies exist to date, the first report focusing on freestanding wires.¹⁵ For 3d transition-metal chains on surfaces, calculations have been performed only for Fe and Co. While Fe chains always order ferromagnetically on the Cu(11n) stepped surfaces,⁸ monoatomic Fe-Co alloy wires on W(970) (Ref. 9) show a strong tendency toward antiferromagnetism due to hybridization with the substrate. Relaxations can also affect the magnetic ground state of 1D systems due to the sensitive influence of substrate-chain interactions. However, they often have not been considered due to computational limitations.

Long before the development of first-principles electronic structure calculations exchange interactions in 3d transition metals (TM's) and their compounds have been widely considered based on the Heitler-London approximation and its formulation for ferromagnets by Heisenberg,¹⁶ known as the Heisenberg model. A cornerstone of this approximation is the

evaluation of the exchange integral J , as given by Heitler and London.¹⁷ For the calculation of this integral there are no analytical models available except for hydrogen.¹⁸ Numerical calculations give unreliable results, with disagreements not only in the magnitude of J , but even its sign.^{19,20} It was pointed out by Herring²¹ that asymptotically the Heitler-London approximation predicts a wrong sign of the exchange energy. Furthermore, Herring²¹ and Landau²² developed a perturbation method based on the surface integral evaluation of J , which was successfully applied to scanning tunneling microscopy²³ and further generalized in order to describe the exchange interactions correctly in the whole range of the distance between the atoms.²⁴

Despite a strong subsequent critique,^{25–27} relying on the Heitler-London expression for the exchange integral J , Bethe made some correct predictions on the sign and magnitude of J for $3d$ TM's.²⁸ Based on Slater's estimates for the mean radii of the $3d$ TM orbitals,²⁹ Bethe suggested a variation of J with interatomic spacing d . He concluded that for small d the exchange integral should be negative and, with increasing d , J approaches zero, becomes positive, reaches a maximum, and exponentially decays to zero. Bethe gave a rough sketch of this behavior, known as the Bethe-Slater (BS) curve,³⁰ which has been applied with some success in the physics of ferromagnetic alloys.^{31,32}

In this paper we present a systematic investigation of the nature of the spin coupling in magnetic monoatomic wires by analyzing the exchange interactions in magnetic metal chains. We focus on $3d$ transition elements which in higher dimensions offer a wide scope of complex magnetic structures. After introducing the method and computational details of our calculations (Sec. I), we first consider the ideal case of freestanding chains of V, Cr, Mn, Fe, and Co (Sec. II). We discuss their magnetic properties and sign of the exchange interaction as a function of the interatomic distance. Surprisingly, we find for V, Cr, and Mn a transition from antiferromagnetic (AFM) to ferromagnetic (FM) coupling with increasing interatomic spacing. Co and Fe wires, in contrast, are ferromagnetic in the entire regime of interatomic distances but display large variations in the strength of the ferromagnetic coupling. The distance-dependent exchange coupling deduced from our calculations is in striking resemblance to the Bethe-Slater curve. Besides a stand-alone interest in the magnetism of these freestanding chains—e.g., in comparison with predictions from much cruder models such as the Bethe-Slater curve—such an investigation gives us a valuable starting point to disentangle the influence of the substrate for chains deposited on a surface.

For this purpose we have investigated the magnetic order in chains deposited on the experimentally promising, unreconstructed (110) surfaces of Cu, Pd, Ag, and NiAl (Sec. III). In particular for the noble metals we expect little influence on the electronic properties of the chain due to weak hybridization with the filled d bands. However, it turns out that due to the reduced symmetry and interaction with the 2D electronic states at the surface, even the weak perturbation of the chains electronic structure is sufficient to turn the magnetic order from ferromagnetic for freestanding Cr and Mn chains to antiferromagnetic for these chains on the surfaces. For V chains the sensitive competition between the exchange inter-

actions within the chain and with the substrate leads to different ground states depending on substrate and lattice spacing.

Special attention is paid to the NiAl(110) substrate, which has been used experimentally as a template to create monoatomic gold chains of up to 20 atoms, and a negligible influence on the gold chains electronic properties has been reported.³³ A subsequent theoretical study confirmed the weak perturbation of the electronic structure also for Mn chains.³⁴ We demonstrate here that the effect on the magnetic properties of monoatomic chains can be dramatic. For example, Cr and Mn chains show weak antiferromagnetic coupling while for Fe and Co the FM and AFM solution are degenerate within 2 meV per chain atom, suggesting the possibility of a more complex, noncollinear ground state due to higher-order spin interactions. We analyze the influence of different substrates in terms of the density of states and discuss the applicability of the generalized Stoner criterion. Finally, we present conclusions and a summary in Sec. IV.

II. COMPUTATIONAL DETAILS

We have performed *ab initio* calculations based on density functional theory (DFT) using the full-potential linearized augmented plane-wave method (FLAPW) in its 1D and 2D formulations as implemented in the FLEUR code.^{35,36} For the exchange-correlation potential we used the rev-PBE generalized gradient approximation to DFT.³⁷

The calculations of freestanding chains have been carried out with the 1D realization of the FLEUR code,³⁵ which allows efficient calculations of chains in a large regime of interatomic spacings. We used 16 k points in one-half of the 1D Brillouin zone (BZ) and k_{\max} of 4.0 a.u.⁻¹.

For calculations of the surface-deposited monoatomic chains we used the film version of the FLEUR code. To simulate the semi-infinite crystal a slab of seven and five substrate layers was used for the fcc (110) and NiAl(110) surfaces, respectively. We used the experimental lattice constants and exploited inversion symmetry by depositing chains on both sides of the substrate slab. Following values for the muffin-tin radii were used: 2.2 a.u. for Cu atoms, 2.3 a.u. for Pd and Ag atoms, 1.7 a.u. for Al atoms, 2.1 a.u. for Ni and chain atoms on NiAl(110), and 2.2 a.u. for the chain atoms on the rest of the surfaces. An in-plane separation between the chains of approximately 15 a.u. (see Fig. 1 for a sketch of the geometrical setup) proved to give reliable results, which was also confirmed by other authors.³⁸ We used values of $k_{\max}=3.6-3.8$ a.u.⁻¹ depending on the surface, achieving consistency in the values of the total energy differences and spin moments. Normally, 24 k points in the irreducible wedge of the 2D BZ were used. If the total energy difference between the FM and AFM states was below 10 meV per chain atom, the reliability of the latter energy difference was checked with 48 k points.

We restricted structural relaxations almost exclusively to the ferromagnetic case with two chain atoms (one on each surface of the slab) in the unit cell, because, as shown later, the magnetic order affects the structural parameters by less than 1%. In this case the reliability of the obtained optimized

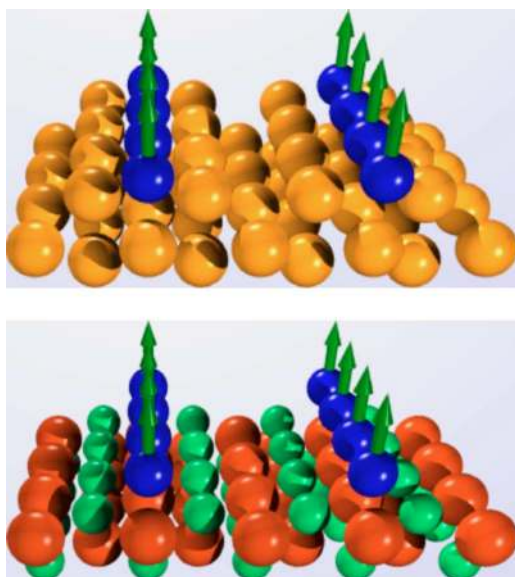


FIG. 1. (Color online) Geometrical setup for $3d$ transition-metal chains deposited on fcc (110) surfaces (top panel) and NiAl(110) (bottom panel). Dark (blue) spheres with arrows indicating the spin moments represent chain atoms. In the upper panel large (gold) spheres represent substrate atoms. In the lower panel large (red) spheres of the substrate denote Ni atoms and small (green) spheres Al atoms.

atomic positions was carefully checked with respect to the number of k points, and we used 12, 24, and 48 in the irreducible wedge of the 2D BZ. If the total energy difference between the FM and AFM states was below 5 meV per chain atom, the structural relaxations were performed also for the AFM configuration. Surface and subsurface layers were relaxed for fcc substrates, while for NiAl(110) only surface-layer relaxations were taken into account.

III. FREE STANDING $3d$ TM CHAINS

We begin our investigation of magnetic exchange interactions in $3d$ transition-metal wires by considering the idealized case of freestanding chains. This way we study the intrinsic magnetic properties of the chains as a function of the $3d$ transition-metal and interatomic spacing d . Based on these calculations we aim at understanding the influence of the substrate on the chain properties, an issue which we elaborate in the next section. We focus on straight chains as our main interest are the properties of chains deposited on surfaces which dictate the chain structure and do not allow effects such as dimerization and zigzag creation. Among the magnetic solutions we consider only the collinear FM and AFM states, while possible noncollinear solutions are beyond the scope of this work.

We find the chains of all considered $3d$ elements, from V to Co, to be strongly magnetic when the distance between the chain atoms is above 4 a.u. and until well beyond 7 a.u. In contrast to $4d$ TM chains,³⁹ in the $3d$ TM chains the atomic orbitals are much more localized and in the whole range of interatomic distances the FM solution coexists with the AFM

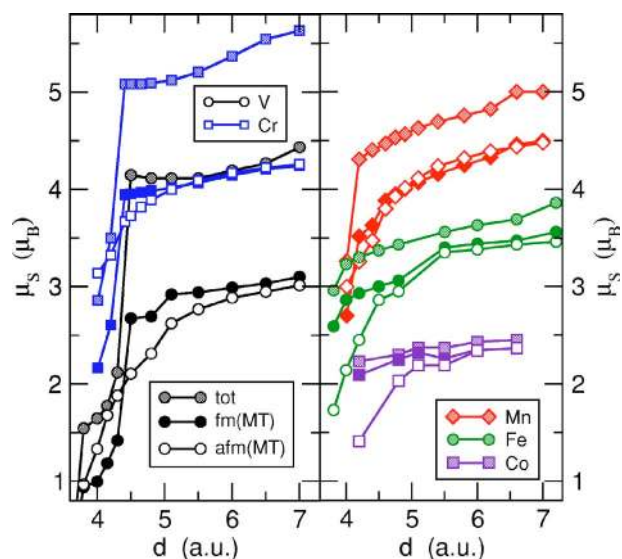


FIG. 2. (Color online) Spin magnetic moments μ_S of freestanding $3d$ transition-metal chains as a function of the interatomic distance d . In the ferromagnetic state the values are given for the total moment (shaded symbols) and the moment integrated in the muffin-tin (MT) spheres (solid symbols). For the antiferromagnetic case only the muffin-tin spin moments are shown (open symbols).

ordering of the local spin moments. The calculated values of the spin moments μ_S are presented in Fig. 2 as a function of the interatomic distance d . At small interatomic distance, the magnetic moments are small due to a strong overlap of the neighboring $3d$ orbitals and rise rapidly with increasing distance, when the intra-atomic exchange begins to dominate. Starting from the interatomic distance in the range of 4–4.5 a.u., depending on the element, the moments reveal a rather smooth behavior. At large d , deviation of μ_S from the atomic value suggests a strong s - d hybridization with significant exchange splitting of the corresponding bands. This effect can be seen, for instance, for V, where the muffin-tin value of $3\mu_B$ is close to that of a free V atom, arising predominantly from localized d electrons, while the remaining contribution to the total moment of around $1\mu_B$ can be attributed to the occupation of the exchange-split delocalized s - d hybridized orbitals.

It is educative, therefore, to compare the spin moment within the muffin-tin sphere of each atom and the total spin moment in the unit cell. Their difference serves as a measure of the spillage of the spin density and, consequently, of the overlap between wave functions of neighboring atoms. It is the largest for V and decreases gradually as we move along the $3d$ series. This is in accordance with the general trend of increasing localization of d orbitals within each transition-metal series. Only for V, Cr, and Mn do we observe that the difference between the muffin-tin (MT) spin moments of the FM and AFM state changes its sign at small interatomic distances within the regime of steeply increasing moments. For all chains, the local FM spin moment is larger than the AFM local moment at intermediate values of d , while the difference between these moments approaches zero with increasing d .

After having established the occurrence of large local magnetic moments due to reduced hopping of $3d$ electrons

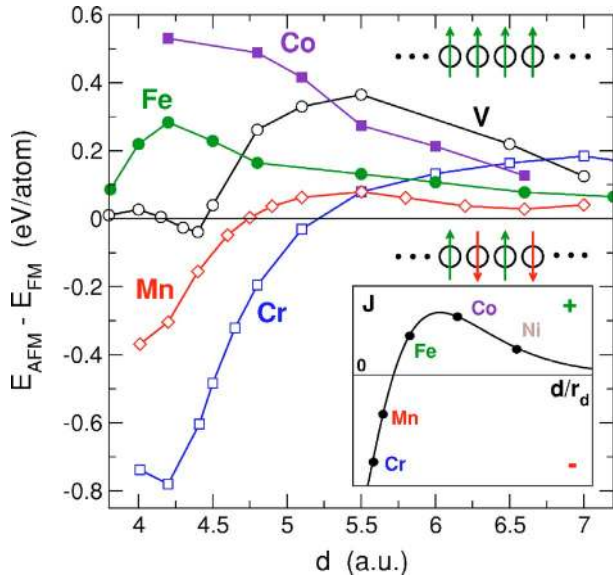


FIG. 3. (Color online) Difference of total energies of the ferromagnetic and the antiferromagnetic solutions as a function of the interatomic distance d for freestanding $3d$ transition-metal chains of V, Cr, Mn, Fe, and Co. The inset shows the Bethe-Slater curve reproduced from Ref. 28—i.e., the exchange integral J as a function of interatomic distance d over the radius of the $3d$ orbitals, r_d (d/r_d ranges from 2.6 for Cr to 3.64 for Co, where d is nearly constant and r_d decreases across the $3d$ series).

and large intra-atomic exchange, we now turn to the magnetic exchange interaction within the chains. In order to study the magnetic coupling, we compare the difference of the total energy of the FM and AFM solutions as a function of d , shown in Fig. 3. Below we refer to this energy difference as $E_{FA}(d)$. For Cr and Mn chains a striking transition from the AFM to the FM state occurs with increasing interatomic distance. In Fe and Co chains, the FM state is favored in the entire regime of d while there is a large variation of the size of the energy difference. V is more complex, showing two transitions. For all chains, E_{FA} approaches zero for large chain atom separation as expected due vanishing wave function overlap.

The occurrence of FM order in Fe and Co wires and in V wires at large d can be understood based on the Stoner criterion because the Fermi energy E_F of the nonmagnetic state is located either in the upper peak (Co, Fe) or the lower peak (V) of the $3d$ band, leading to a large density of states (DOS). The AFM ground state of Cr and Mn chains at small interatomic distances has a similar reason as that reported for Mo and Tc chains.^{8,39} Within the concept of band magnetism, it is due to a position of E_F in the center of the d bands and a low DOS at E_F in the nonmagnetic case.^{8,39}

In contrast to chains of the late $4d$ and $5d$ transition metals, where a transition from an AFM to a FM state has not been observed,⁸ the change of the magnetic ground state of Cr and Mn occurs at distances of 5.21 and 4.75 a.u., respectively. This transition, happening in the regime of nearly constant spin moments with a negligible difference between the local FM and AFM values, can be traced back to a change in the sign of the exchange interaction. For V, an interplay of

the intra-atomic exchange energy due the steep rise of the moment with different moments of the FM and AFM configuration, $\mu_S^{FM}(d)$ and $\mu_S^{AFM}(d)$, with a change in the sign of the exchange interaction, leads to a peculiar behavior of $E_{FA}(d)$: with magnetic ground-state transitions happening twice, at 4.16 a.u. and 4.45 a.u.

Interestingly, we observe that the general form of the total energy difference $E_{FA}(d)$ in the freestanding $3d$ TM chains resembles that predicted by the BS curve for the exchange integral $J(d)$ (see inset in Fig. 3). Within the Heisenberg model restricted to nearest-neighbor coupling, the total energy difference can be obtained from the exchange integral:

$$E_{FA}(d) = 4J(d)S(d)^2, \quad (1)$$

where $S(d)$ is the spin moment of each chain atom. Assuming a constant value of $S(d)$ as a function of d for the moment, we expect a similar functional form of the energy difference and the exchange integral. [This is a good approximation in a wide range of interatomic distances d ; cf. Fig. 2. Using the values obtained for the spin moments as a function of d , we can explicitly calculate the exchange constant $J(d)$ leading to the same qualitative conclusions as discussed below.]

Concerning the comparison, we find for V, Cr, Mn, and Fe chains a maximum of the total energy difference and a drop to zero at larger d in agreement with the BS curve. For Cr the decay is outside the regime shown in the graph while for Co the maximum is at smaller values of d . In addition, Cr and Mn display the mentioned transition from an AFM to a FM state which is a key feature of the BS curve. The interatomic distance d_0 of the transition is proportional to the radial extent of the $3d$ orbitals in the Bethe-Slater theory. (Note that d is approximately constant for the given transition metals on the BS curve.) The calculated transition point shifts to the left from Cr to Mn to Fe in agreement with a decreasing radius of the $3d$ shell. (V is an exceptional case as discussed above and for Co the transition would occur at a value of d where the chain is nonmagnetic.)

We can even make a more quantitative comparison. Considering only Cr, Mn, Fe, and Co chains, we find that up to a distance of 5.5 a.u., Cr is more antiferromagnetic than Mn and Co is more ferromagnetic than Fe. Within the nearest-neighbor Heisenberg model we can translate this into $J_{Cr}(d) < J_{Mn}(d)$ and $J_{Co}(d) > J_{Fe}(d)$ since $S_{Cr} \approx S_{Mn}$ and $S_{Fe} > S_{Co}$ (cf. Figs. 2 and 3). This is in accordance with the BS curve as well, after noticing that the positions of the elements on the latter curve are given at roughly the same interatomic distance d of 4.72–4.76 a.u.²⁹

The direct comparison of the exchange integral $J(d)$ and the total energy difference $E_{FA}(d)$ is only valid within the nearest-neighbor Heisenberg model, and exchange interactions beyond nearest neighbors as well as interactions beyond the Heisenberg model—e.g., biquadratic terms—could play a role in the chains. The qualitative agreement of our calculation with the Bethe-Slater curve suggests a dominant nearest-neighbor exchange interaction. However, we cannot scale the curves to a single, unique function, which indicates the presence of other exchange mechanisms depending on the specific $3d$ element.

Besides being an interesting observation our confirmation of the Bethe-Slater-like behavior of the exchange interaction as a function of interatomic distance in low-dimensional itinerant magnetism could be useful. It can serve as an ansatz and be a benchmark for further analytical and numerical endeavors in estimating the exchange integral²⁴ and a starting point to explore the limits of the Heisenberg model for chains and clusters of transition metals.¹²

We speculate that the unexpected behavior of the magnetic coupling, in particular the magnetic ground-state transition at specific interatomic distances, could even be observed in magnetic breakjunctions or by using nanowires or carbon nanotubes as a template for monoatomic chain growth.

IV. 3d TM CHAINS ON SURFACES

In the previous section we have revealed a Bethe-Slater-type behavior of the exchange interaction in monoatomic 3d transition-metal wires. In the following we investigate how far the magnetic properties of such ideal freestanding chains can be conserved after deposition on a surface. Obviously, interactions between chain and surface atoms come into play and various hybridization-driven effects such as symmetry reduction and indirect exchange interactions will affect the magnetic ground state. Whether we can deduce the magnetic properties of the composite system from its constituents is not clear *a priori*.

A related subject and conceptual starting point for our study are monolayers of 3d TM's on surfaces. In this field we can roughly distinguish two classes of (nonmagnetic) substrates: weakly and strongly hybridizing. The first class, besides insulating materials, includes, for instance, noble metals such as Cu and Ag and can be characterized by a small monolayer-substrate interaction of d electrons. In this case, the magnetic order is determined by exchange interactions within the two-dimensional monolayer itself and does not change from the unsupported monolayers.⁴⁰ In contrast, 5d TM's such as tungsten or iridium with their delocalized 5d orbitals are typical examples of the second class of materials. Such surfaces strongly influence the magnetic order of the overlayer, and the magnetic ground state depends sensitively on the composite monolayer-substrate system.^{14,41–43} For a monoatomic chain, however, the number of nearest neighbors is significantly smaller than for a monolayer, and one could expect interactions with the substrate to become comparable to those within the chain itself, if not dominant, even for the substrates from the first class. In this section we confirm this notion based on our *ab initio* calculations.

In order to investigate the effect of a substrate on the magnetic state of the 3d TM chains, we have chosen the experimentally promising (110) surfaces of fcc Cu, Ag, Pd, and bcc NiAl. These unreconstructed surfaces provide trenches for the growth of the chains (see Fig. 1) and thereby may enable the creation of monoatomic chains by atom manipulation as well as by self-assembly. In our calculations the chain atoms are located in the hollow sites of the surface layer above the subsurface layer atoms as shown in Fig. 1. In this geometry every chain atom possesses two chain atoms as

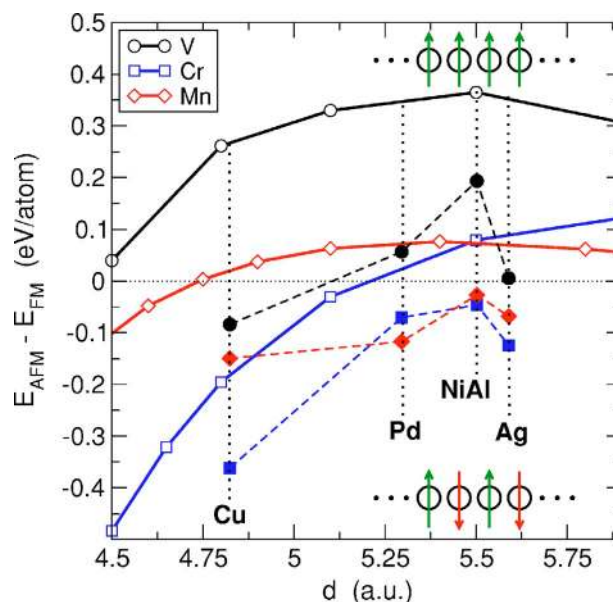


FIG. 4. (Color online) Difference in total energy between the FM and the AFM solution (per chain atom) of V, Cr, and Mn chains deposited on the (110) surfaces of Cu, Pd, Ag, and NiAl (solid symbols and dashed lines) and, for comparison, the values of Fig. 3 for the freestanding configuration (open symbols and solid lines). The interatomic spacing on the Cu, Pd, NiAl, and Ag(110) surface is indicated by dotted lines.

well as five surface atoms as nearest neighbors. In a previous theoretical study³⁴ it has been demonstrated that the electronic properties of Mn, Ni, Au, and Cu chains are only weakly perturbed in this configuration on NiAl(110); however, the magnetic order was not considered. The interatomic distance in the chains is dictated by the substrate lattice constant. We keep this constant at its experimental values—i.e., 4.82 a.u. for Cu, 5.30 a.u. for Pd, 5.59 a.u. for Ag, and 5.50 a.u. for NiAl—relaxing the rest of the structural parameters, as described in Sec. II. These values are well suited to scan the interesting regime of interatomic spacings of the freestanding chains, in particular to check whether the transition from AFM to FM can be conserved on a surface.

We initially focus on chains of V, Cr, and Mn because these show a FM-AFM magnetic order transition with interatomic spacing, and later on we complete our calculations by considering Fe and Co chains on Cu(110) and NiAl(110). As in the previous section we discuss the total energy difference between the FM and AFM solutions defined as E_{FA} , shown in Fig. 4. In comparison to the freestanding chains, we observe a striking shift in the energy difference in favor of antiferromagnetic order. For Cr and Mn wires this shift is 100–200 meV per atom and leads to an AFM solution on all considered surfaces. However, the general monotonic increase of E_{FA} as a function of d up to 5.5 a.u. observed for the freestanding chains is preserved and especially visible for Cr. Clearly, there is a competition between ferromagnetic intrachain coupling and antiferromagnetic coupling due to the substrate. On the (110) surface of NiAl this competition results in a very weak overall antiferromagnetic coupling.

The magnetic order in V chains is more sensitive to the specific surface. For a freestanding chain the FM solution is

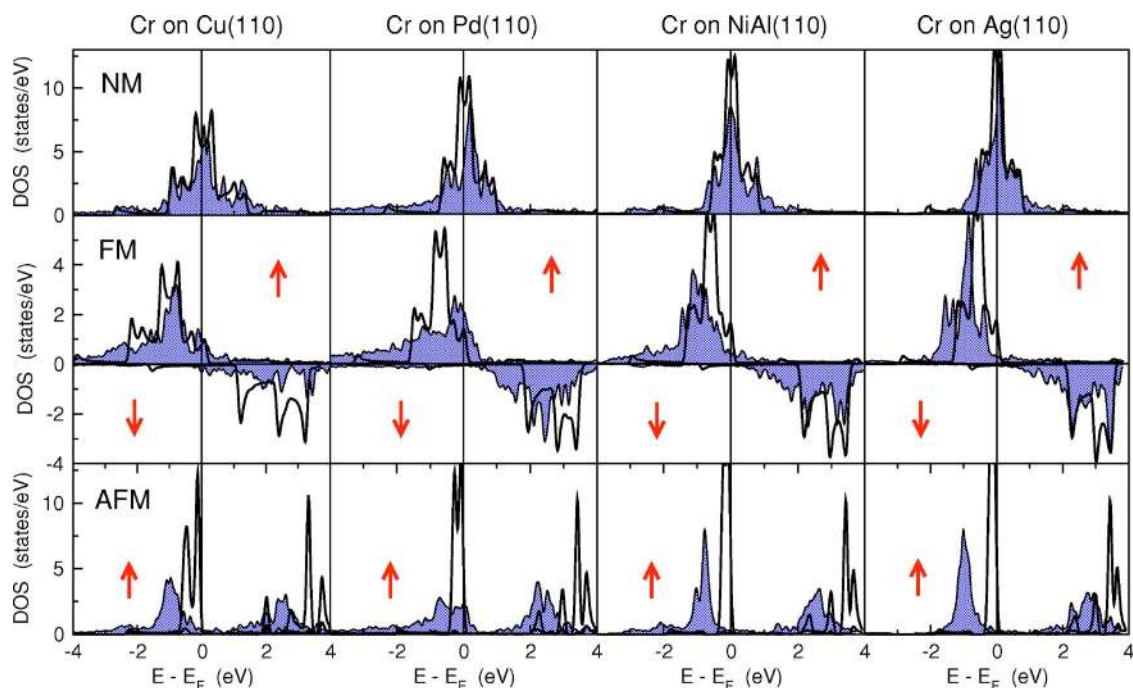


FIG. 5. (Color online) Densities of states (DOS) for Cr chains on the (110) surfaces of Cu, Pd, NiAl, and Ag in the nonmagnetic (top panel), ferromagnetic (middle panel), and antiferromagnetic (bottom panel) states. Arrows indicate the spin-up and spin-down channels. Blue shaded areas denote the local DOS of the Cr atoms for chains on the surface while black lines correspond to freestanding Cr chains.

favorable by a very large energy; however, the interaction with the surface shifts the entire curve by about 300 meV per atom which leads to a transition to an AFM state on Cu(110). At a slightly larger interatomic distance on the Pd(110) surface, the FM state is recovered. On NiAl(110) the total energy difference rises even more in favor of the FM solution. The sensitive influence of the specific surface electronic structure on the magnetic coupling is apparent from the case of Ag(110). While the freestanding V chain has a strong tendency towards a FM state the competition with the chain-surface interaction leads to the peculiar situation of a nearly degeneracy of the FM and AFM states. In such a situation, magnetic states beyond these simple collinear states need to be considered since magnetic interactions beyond nearest neighbors might play a role.

A more detailed analysis and understanding of the impact of the substrate on the magnetic coupling in the deposited chains can be obtained from the DOS. We choose Cr chains as an example, and Fig. 5 displays the local DOS of the Cr atoms on the four considered substrates in comparison with the freestanding geometry at the corresponding interatomic distance. Starting with the DOS of the nonmagnetic state, shown in the upper row of Fig. 5, we observe the characteristic 1D van Hove singularities in the $3d$ band of the freestanding chains. For Cr the Fermi energy is between two singularities approximately in the center of the $3d$ band. Within a generalized Stoner picture this position of the Fermi energy in combination with a relatively wideband DOS leads to an AFM ground state. As the interatomic spacing is increased—i.e., from left to right in Fig. 5—the bandwidth decreases and the DOS rises sharply at the Fermi energy. While the Fermi energy is still in the center of the $3d$ band

the enhanced DOS results in an instability towards a FM solution. This transition from an AFM to a FM state leads to the observed Bethe-Slater-type behavior discussed in the previous section.

Next we turn to the nonmagnetic deposited Cr chains. Due to s - d hybridization of surface and chain states, the DOS spills out from the $3d$ band of Cr which slightly increases the bandwidth. More important, however, is the smearing out of the sharp features which were present in the DOS of the freestanding chains. Because of the reduced symmetry at the surface and interaction with the two-dimensional bath of the surface electrons, band degeneracies are lifted and the van Hove singularities at the Fermi energy due to the hybridization of d_{xy} and $d_{x^2-y^2}$ states in the free chains disappear. This reduction of the DOS at the Fermi energy causes the transition to AFM order for Cr chains on the surfaces.

While the Stoner picture suggests a simple explanation of the magnetic order in these systems one should note that the magnetic solutions (see middle and bottom rows of Fig. 5) display additional hybridization effects due to the exchange splitting of the DOS. These are particularly strong for the AFM solution. For freestanding chains there is little hybridization between nearest neighbors due to the antiparallel spin alignment and the DOS consists of sharp resonance features. On a surface these peaks broaden into bands. Such hybridization effects in combination with surface relaxations may influence the magnetic ground state of a specific chain-surface system. E.g., for Cr and Mn chains on NiAl(110) the total energy difference between FM and AFM state is quite small due to the competition of intrachain and chain-surface interactions and sensitive to other influences.

In low-dimensional systems structural relaxations can be crucial due to the reduced coordination number and have

TABLE I. Relaxations of the metal chains on (110) surfaces of Cu, Pd, Ag, and NiAl. For the fcc (110) surfaces the following parameters are given: ΔY , change in distance of the atom of the surface layer to the chain axis (x axis) along the y axis (perpendicular to the chain); ΔZ_1 , change in distance along the z axis between the chain atom and the surface layer; ΔZ_2 , change in distance along the z axis between the chain atom and the closest atom of the subsurface layer; d_1 (d_2), distance between the chain atom and the closest atom of the surface (subsurface) layer. For the NiAl(110) surface the following parameters are presented: ΔY_{Al} , change in distance of the Al atom of the surface layer to the chain axis along the y axis; $\Delta Z_{M-\text{Al}}$ ($\Delta Z_{M-\text{Ni}}$), change in distance along the z axis between the chain atom and the Al (Ni) atom of the surface layer; $d_{M-\text{Al}}$ ($d_{M-\text{Ni}}$), distance between the chain atom and the Al (Ni) atom of the surface layer. All the values, except when specified differently, are given in atomic units, “+” (“-”) mean increase (decrease) in respective distance, as compared to the unrelaxed value. The unrelaxed values of d_1 and d_2 are the nearest-neighbor distances of the corresponding unrelaxed substrates—i.e., 4.824, 5.295, and 5.590 a.u. for Cu, Pd, and Ag, respectively. The unrelaxed values of $d_{M-\text{Al}}$ and $d_{M-\text{Ni}}$ for NiAl(110) are 5.502 and 4.765 a.u., respectively.

	ΔY	ΔZ_1	ΔZ_2	d_1 (%)	d_2 (%)
Cu(110)					
V	+0.13	+0.17	+0.18	+3.7	+3.7
Cr	+0.12	+0.22	+0.22	+4.0	+4.6
Mn	+0.13	+0.04	+0.08	+2.3	+1.7
Fe	+0.11	-0.18	-0.08	-0.2	-1.7
Co	+0.10	-0.30	-0.21	-1.4	-4.3
Pd(110)					
V	-0.07	-0.85	-0.62	-7.9	-11.8
Cr	-0.00	-0.66	-0.45	-5.6	-8.5
Mn	-0.02	-0.65	-0.45	-5.9	-8.5
Ag(110)					
V	+0.04	-0.25	-0.13	-1.6	-2.3
Cr	+0.03	-0.25	-0.15	-1.8	-2.7
Mn	+0.03	-0.58	-0.33	-4.4	-5.8
NiAl(110)					
	ΔY_{Al}	$\Delta Z_{M-\text{Al}}$	$\Delta Z_{M-\text{Ni}}$	$d_{M-\text{Al}}$ (%)	$d_{M-\text{Ni}}$ (%)
V	+0.07	-0.070	+0.17	+0.0	+3.0
Cr	+0.10	+0.04	+0.17	+1.3	+3.0
Mn	+0.08	-0.10	-0.11	-0.2	-1.8
Fe (FM)	+0.10	-0.28	-0.38	-6.4	-6.3
Fe (AFM)	+0.08	-0.61	-0.32	-6.4	-5.4
Co (FM)	+0.05	-0.80	-0.38	-8.9	-6.4
Co (AFM)	+0.05	-0.75	-0.35	-8.4	-5.9

therefore been taken into account for the chains on surfaces. The results of the relaxations are summarized in Table I. We observe significant changes of the lateral and vertical positions of the chain, surface, and subsurface atoms in many cases. It is useful to focus in particular on the change of the nearest-neighbor distances (d_1 and d_2). On the Cu(110) surface, the V, Cr, and Mn chains relax outward from the Cu

surface and the surface Cu atoms shift slightly away from the chain axis to reduce the compression of the $4s$ -electron gas, and the nearest-neighbor distances increase by up to 4.5%. Fe and Co chains, with less extended $3d$ orbitals, on the other hand, relax considerably inward but the surface Cu atoms move away from the chain axis and the nearest-neighbor distances d_1 are only slightly changed. The Ag(110) surface possesses a much larger lattice constant, in comparison, and consequently also the early $3d$ TM chains of V, Cr, and Mn display strong inward relaxations while the Ag surface atoms shift only by small amounts.

On the Pd(110) surface, in contrast, there is strong hybridization and bonding of Pd $5d$ and chain $3d$ states and all chains relax inward by large amounts and the bond lengths are much reduced. This chain-surface interaction is also reflected in a large reduction of the chain magnetic moments; cf. Table II.

The NiAl(110) surface is structurally more complex due to the interaction with two different chemical species of the surface. The bond length to the Al atoms changes in a similar fashion as observed above on the Cu and Ag surfaces. For V, Cr, and Mn chains the distance changes only slightly while for Fe and Co chains it decreases by 6%–8%. (Note that there is only little dependence of the relaxation on the magnetic state for Fe and Co chains, supporting our decision to relax only critical systems in both FM and AFM configurations.) The distance to the Ni atoms increases for V and Cr, while large reductions are found for Fe and Co. In general, we find that Co suffers the strongest interactions.

Another indicator of the chain-surface interaction and its influence on the chain magnetism is the change of the spin moment given in Table II for the $3d$ TM chains. Among the three elements, V is prone to the largest interaction with the substrate leading to large reductions of the spin moment; e.g., on the Cu(110) and Pd(110) surface it decreases by almost half the value of the freestanding chain in the FM state. On NiAl and Ag, with larger nearest-neighbor distances, the hybridization between chain and surface is smaller and the spin moments change much less. For Cr and Mn the changes of the spin moment are in general much smaller. The relatively large reduction of the Cr total moment (in the unit cell) on Pd(110) is due to the antiferromagnetic coupling to the surface Pd atoms. In contrast, the coupling is ferromagnetic for Mn chains and the Mn moment is affected only weakly. For Mn the spin moments remain close to $4\mu_B$ on all surfaces and for all magnetic configurations. Fe and Co spin moments are influenced more strongly than those of Mn, but still the reduction in their values reaches at most $0.5\mu_B$. In conclusion, the size of the magnetic moments is influenced weakly by the interaction with the surfaces while the magnetic order in the chains depends sensitively on it.

In order to take a different perspective on the mechanism responsible for the drastic changes in the ground state of the supported chains we investigate their magnetism as a function of the band filling on Cu(110) and NiAl(110), Fig. 6. The interaction with the NiAl(110) surface shifts the entire total energy curve by an almost constant energy towards the AFM state. The largest influence of the surface is seen for Co, in agreement with the strongest relaxations; cf. Table I.

TABLE II. Magnetic spin moments of V, Cr, Mn, Fe, and Co chains on the (110) surfaces of Cu, Pd, NiAl, and Ag in the ferromagnetic (FM), and antiferromagnetic (AFM) states. In the FM state the total moment in the unit cell [FM (tot)], the moment within the muffin-tin sphere around the chain atoms [FM (mt)], and the muffin-tin moment of the closest surface atom [Surf. (mt)] are given. In the AFM state only the muffin-tin moment can be given. Values in brackets correspond to those for the freestanding chains on the substrate-imposed interatomic distance. All magnetic moments are given in units of μ_B .

	Cu(110)	Pd(110)	NiAl(110)	Ag(110)
V				
FM (tot)	2.38 (4.12)	1.03 (4.11)	3.82 (4.12)	3.62 (4.13)
FM (mt)	1.72 (3.00)	1.64 (2.93)	2.51 (2.94)	2.67 (2.95)
Surf. (mt)	0.02	-0.27	0.28	0.03
AFM (mt)	1.95 (2.56)	1.45 (2.73)	2.36 (2.80)	2.54 (2.83)
Cr				
FM (tot)	4.19 (5.09)	2.46 (5.16)	4.83 (5.20)	4.73 (5.22)
FM (mt)	3.43 (3.98)	3.26 (4.04)	3.67 (4.07)	3.87 (4.08)
Surf. (mt)	0.05	-0.30	0.22	0.02
AFM (mt)	3.41 (3.89)	3.22 (4.05)	3.62 (4.09)	3.81 (4.10)
Mn				
FM (tot)	4.11 (4.54)	4.60 (4.66)	4.72 (4.72)	4.57 (4.73)
FM (mt)	3.69 (3.97)	4.00 (4.12)	3.93 (4.18)	4.05 (4.20)
Surf. (mt)	0.04	0.13	0.24	0.02
AFM (mt)	3.75 (3.98)	3.96 (4.20)	3.92 (4.27)	4.12 (4.29)
Fe				
FM (tot)	3.05 (3.43)		3.28 (3.56)	
FM (mt)	2.92 (3.06)		2.89 (3.40)	
Surf. (mt)	0.03		0.29	
AFM (mt)	2.82 (2.95)		2.88 (3.35)	
Co				
FM(tot)	1.75 (2.30)		1.98 (2.37)	
FM (mt)	1.77 (2.25)		1.81 (2.26)	
Surf. (mt)	0.02		0.17	
AFM (mt)	1.66 (2.03)		1.82 (2.19)	

While V maintains its FM configuration, for Cr and Mn the interaction causes a transition of the ground state from FM to AFM. For the prototypical ferromagnets Fe and Co, the interaction with the surface is not sufficient to induce AFM coupling; however, the FM and AFM states are almost degenerate. (In our calculation, Fe is slightly AFM while Co is FM; however, the energy differences amount to only 2 meV per chain atom.) Note that the chains are still strongly magnetic with moments of $2.89\mu_B$ and $1.81\mu_B$ for Fe and Co, respectively. Such a significant weakening of the nearest-neighbor FM coupling in the chain could lead to a more complex magnetic ground state such as a spin-spiral state due to interactions beyond nearest neighbors or higher-order spin interactions. On Cu(110), the behavior is different and resembles the typical behavior of 2D films on surfaces. In

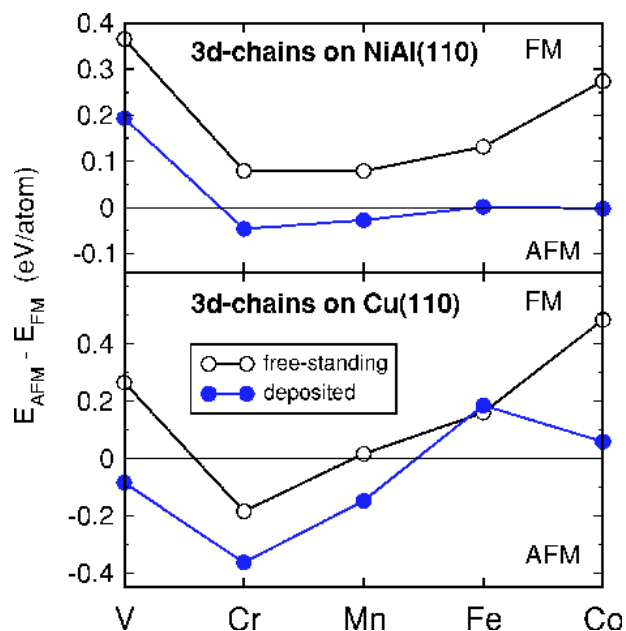


FIG. 6. (Color online) Difference in total energy between the FM and AFM solutions for 3d transition-metal chains in the freestanding configuration and after depositing on the NiAl(110) (top panel) and the Cu(110) (bottom panel) surfaces. The freestanding wires have been calculated at the interatomic spacing corresponding to the respective surface.

particular, we observe that the early 3d TM's show AFM order while the late 3d TM's are FM with the transition between Mn and Fe.⁴⁰

More insight into the chain-surface interaction can be obtained from the densities of states, presented in Fig. 7 for chains on NiAl(110). In the nonmagnetic calculation (upper panels), we observe that the V and Cr *d* bands are rather high in energy and overlap only with the strongly dispersive *sp* states of the Al atoms near the Fermi energy. The low DOS of Al prevents major modifications in the *d* bands of V and Cr, and characteristic features and the bandwidths are nearly preserved. At the end of the 3d series in contrast, the *d* bands of Fe and Co are lower in energy due to larger band filling and reach the energetic position of the high DOS of the surface Ni atoms. The hybridization is consequently strong, and distinctive peaks of the freestanding chain DOS are smeared out. For the magnetic solutions, the exchange splitting pushes the chains *d* bands down in energy, effectively increasing the overlap with the *d* states of surface Ni, smoothing out the freestanding chains DOS significantly (this effect is in particular clear for AFM Co). Therefore, the simple Stoner picture, where the DOS of the spin-polarized chain could be obtained by a simple shift of the nonmagnetic DOS, cannot provide a full explanation of the magnetic ground state. In addition, the large exchange splitting of the chains 3d bands causes a large spin polarization at the Fermi energy for Mn, Fe, and Co chains.

V. CONCLUSIONS

We have performed *ab initio* calculations to investigate the magnetic order and exchange interactions of monoatomic

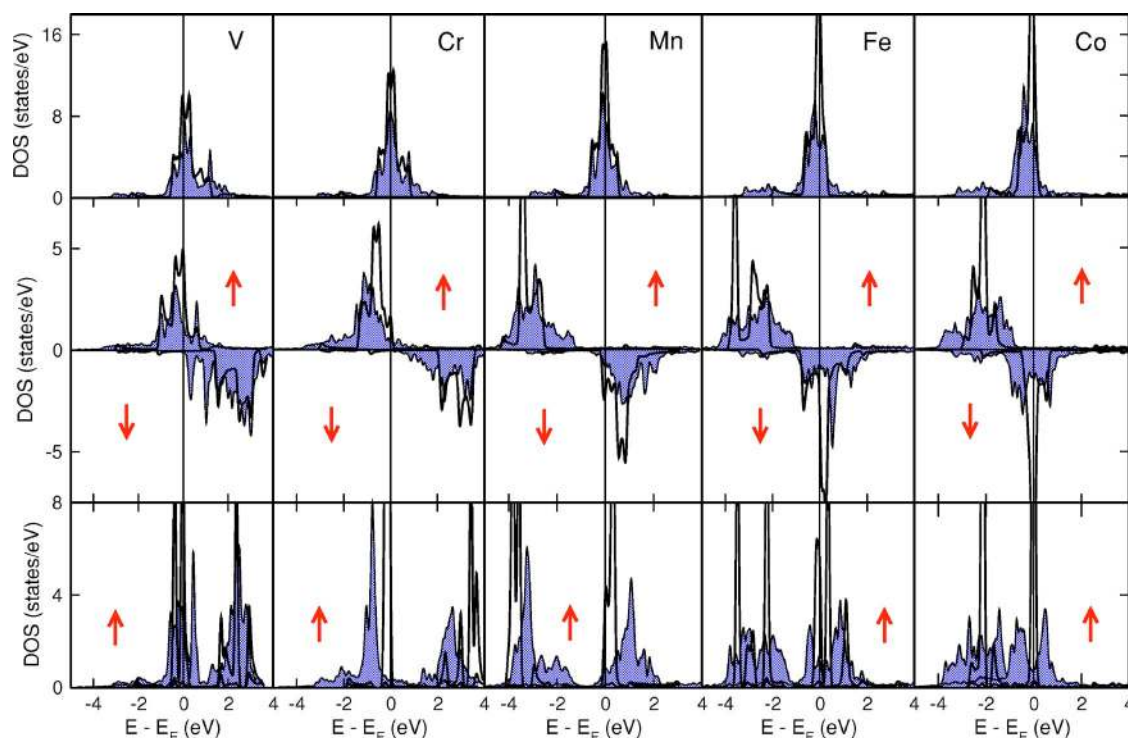


FIG. 7. (Color online) Densities of states (DOS) for $3d$ TM chains on NiAl(110) in the nonmagnetic (top panel), ferromagnetic (middle panel), and antiferromagnetic (bottom panel) states. Arrows indicate the spin-up and spin-down channels. Shaded areas denote the local DOS of the chain atoms. For comparison, solid black lines indicate the local DOS of the freestanding chains.

chains of the $3d$ transition metals V, Cr, Mn, Fe, and Co as a function of interatomic distance with and without substrates. As trial substrates for this purpose we have chosen the experimentally promising (110) surfaces of Cu, Pd, Ag, and NiAl.

For the freestanding chains we have found the expected strong tendency towards magnetism—e.g., the occurrence of large magnetic moments and stable FM and AFM solutions. We find a transition from antiferromagnetic to ferromagnetic coupling with interatomic distance for V, Cr, and Mn while Fe and Co are ferromagnetic within the entire regime. We deduce the exchange coupling from our calculations and find that the functional dependence on interatomic spacing closely resembles the Bethe-Slater curve for all these elements.

For chains on surfaces a large shift in the exchange coupling towards antiferromagnetism occurs. Even on the NiAl(110) surface, a favorable template for chain growth with negligible effect on the chains intrinsic electronic properties, the reduction in the energy difference between FM and AFM states is significant. This results in a ground-state transition from FM to AFM for Mn and Cr. For Fe and Co, which suffer a stronger interaction with the NiAl surface than

the early $3d$ TM's, the nearest-neighbor FM exchange coupling between the neighboring spins is significantly weakened. Under such conditions, higher-order spin interactions or exchange interactions beyond nearest neighbors may determine the final ground state which could be more complex than the simple collinear state.

Given the localized nature of the $3d$ orbitals and the strong intra-atomic magnetism in $3d$ TM chains with large local spin moments, we characterize the magnetism in these chains as supple—i.e., locally strong with the coupling between the neighboring spins being easily modified by interactions with the surroundings. The delicacy of the chains exchange interactions suggests a search for new criteria in evaluating the influence of the substrate on the magnetism in chains and opens a quest for new types of surfaces, which do not significantly affect the magnetic coupling between the deposited atoms.

ACKNOWLEDGMENTS

Financial support of the Stifterverband für die Deutsche Wissenschaft and the Interdisciplinary Nanoscience Center Hamburg is gratefully acknowledged.

*Electronic address: ymokrous@physnet.uni-hamburg.de

- ¹N. Zabala, M. J. Puska, and R. M. Nieminen, *Phys. Rev. Lett.* **80**, 3336 (1998).
- ²A. Auyela, H. Rabiger, M. J. Puska, and R. M. Nieminen, *Phys. Rev. B* **66**, 035417 (2002).
- ³P. Gambardella, A. Dallmeyer, K. Maiti, M. C. Malagoli, W. Eberhardt, K. Kern, and C. Carbone, *Nature (London)* **416**, 301 (2002).
- ⁴A. B. Shick, F. Maca, and P. M. Oppeneer, *Phys. Rev. B* **69**, 212410 (2004).
- ⁵B. Újfalussy, B. Lazarovits, L. Szunyogh, G. M. Stocks, and P. Weinberger, *Phys. Rev. B* **70**, 100404(R) (2004).
- ⁶S. Baud, C. Ramseyer, G. Bihlmayer, and S. Blügel, *Phys. Rev. B* **73**, 104427 (2006).
- ⁷V. Bellini, N. Papanikolaou, R. Zeller, and P. H. Dederichs, *Phys. Rev. B* **64**, 094403 (2001).
- ⁸D. Spišák and J. Hafner, *Phys. Rev. B* **67**, 214416 (2003).
- ⁹D. Spišák and J. Hafner, *Phys. Rev. B* **70**, 014430 (2004).
- ¹⁰L. Yan, M. Przybylski, Y. Lu, W. H. Wang, J. Barthel, and J. Kirschner, *Appl. Phys. Lett.* **86**, 102503 (2005).
- ¹¹L. Hammer, W. Meier, A. Schmidt, and K. Heinz, *Phys. Rev. B* **67**, 125422 (2003).
- ¹²C. Hirjibehedin, C. Lutz, and A. Heinrich, *Science* **312**, 1021 (2006).
- ¹³H. J. Lee, W. Ho, and M. Persson, *Phys. Rev. Lett.* **92**, 186802 (2004).
- ¹⁴K. von Bergmann, S. Heinze, M. Bode, E. Y. Vedmedenko, G. Bihlmayer, S. Blügel, and R. Wiesendanger, *Phys. Rev. Lett.* **96**, 167203 (2006).
- ¹⁵M. Weinert and A. J. Freeman, *J. Magn. Magn. Mater.* **38**, 23 (1983).
- ¹⁶W. Heisenberg, *Z. Phys.* **49**, 619 (1928).
- ¹⁷W. Heitler and F. London, *Z. Phys.* **44**, 455 (1927).
- ¹⁸Y. Sugiura, *Z. Phys.* **45**, 484 (1927).
- ¹⁹J. Slater, *Rev. Mod. Phys.* **25**, 199 (1953).
- ²⁰R. Stuart and W. Marshall, *Phys. Rev.* **120**, 353 (1960).
- ²¹C. Herring, *Rev. Mod. Phys.* **34**, 631 (1962).
- ²²L. Landau and E. Lifshitz, *Kvantovaya Mekhanika* (Fizmatlit, Moscow, 1963).
- ²³C. Chen, *J. Phys.: Condens. Matter* **3**, 1227 (1991).
- ²⁴C. J. Chen and R. Wiesendanger, *Phys. Rev. B* **74**, 113102 (2006).
- ²⁵J. V. Vleck, *Rev. Mod. Phys.* **25**, 220 (1953).
- ²⁶C. Zener, *Phys. Rev.* **81**, 440 (1951).
- ²⁷J. Slater, *Phys. Rev.* **49**, 537 (1936).
- ²⁸A. Sommerfeld and H. Bethe, *Handbuch der Physik* (Springer, Berlin, 1933).
- ²⁹J. Slater, *Phys. Rev.* **36**, 57 (1930).
- ³⁰R. Bozorth, *Ferromagnetism* (Van Nostrand, Princeton, 1951).
- ³¹Q. Pankhurst, L. Barquin, J. Wicks, R. McGreevy, and M. Gibbs, *J. Phys.: Condens. Matter* **9**, L375 (1997).
- ³²K. Gallaher, M. Willard, V. Zabenkin, D. Laughlin, and M. McHenry, *J. Appl. Phys.* **85**, 5130 (1999).
- ³³T. M. Wallis, N. Nilius, and W. Ho, *Phys. Rev. Lett.* **89**, 236802 (2002).
- ³⁴A. Calzolari and M. B. Nardelli, *Phys. Rev. B* **72**, 045416 (2005).
- ³⁵Y. Mokrousov, G. Bihlmayer, and S. Blügel, *Phys. Rev. B* **72**, 045402 (2005).
- ³⁶URL <http://www.flapw.de>
- ³⁷Y. Zhang and W. Yang, *Phys. Rev. Lett.* **80**, 890 (1998).
- ³⁸J. Hong, *Phys. Rev. B* **73**, 092413 (2006).
- ³⁹Y. Mokrousov, G. Bihlmayer, S. Heinze, and S. Blügel, *Phys. Rev. Lett.* **96**, 147201 (2006).
- ⁴⁰S. Blügel, B. Drittler, R. Zeller, and P. Dederichs, *Appl. Phys. A: Solids Surf.* **49**, 547 (1989).
- ⁴¹D. Spišák and J. Hafner, *Phys. Rev. B* **70**, 195426 (2004).
- ⁴²A. Kubetzka, P. Ferriani, M. Bode, S. Heinze, G. Bihlmayer, K. von Bergmann, O. Pietzsch, S. Blügel, and R. Wiesendanger, *Phys. Rev. Lett.* **94**, 087204 (2005).
- ⁴³P. Ferriani, S. Heinze, G. Bihlmayer, and S. Blügel, *Phys. Rev. B* **72**, 024452 (2005).